

Miniaturized Folded Antenna with Improved Matching Characteristic for mm-wave Detections

Saad G. Muttlak

Department of Electrical and
Electronic Engineering
The University of Manchester
Manchester, United Kingdom
saad.muttlak@manchester.ac.uk

M. Sadeghi

Advanced Hall Sensors Ltd
Manchester, United Kingdom
mohammadreza.sadeghi@ahsLtd.com

Kawa Ian

Integrated Compound Semiconductors
Manchester, United Kingdom
kawan.ian@icsld.com

Mohamed Missous

Department of Electrical and
Electronic Engineering
The University of Manchester
Manchester, United Kingdom
m.missous@manchester.ac.uk

Abstract—This work reports on the design and analysis of a folded antenna operating at mm-wave frequencies. Prior to this, several folded antennas operating at 7, 9 and 10GHz frequencies were used to validate the simulation procedure performed. A mm-wave folded antenna with a resonant frequency of 39GHz was then simulated. A relatively small antenna geometry was achieved without sacrificing its gain and other crucial characteristics. A 3.5dB gain and 4.6dBi directivity were obtained with a frequency bandwidth reaching 780MHz. The main and secondary arm widths of the folded antenna are key in determining the real and imaginary parts of the antenna impedance, providing a degree of freedom for the designer to get the antenna well-matched with the subsequent integrated circuit. This provides useful features including the capability of reducing the overall antenna dimensions and avoiding matching circuits.

Keywords—folded antenna, mm-wave, integrated detector, CST-Microwave Studio

I. INTRODUCTION

In recent years, increased interest in the mm-wave regime and corresponding applications has been witnessed as reflected in the growing demand for high-speed wireless network systems[1]. The forthcoming fifth-generation (5G) mobile technology is key in enabling the >10Gbps hotspot areas reserved for enhanced mobile broadband scenarios[2]. According to the third-generation partnership project (3GPP), one of the present licensed 5G mm-wave frequencies is the coded n260 band ranging from 37 to 40GHz[3]. Other candidate frequency bands at 26, 28, 38 and 39GHz are also endorsed by the United Kingdom's regulator and competition authority, Ofcom[4]. Due to the high lossy path and atmospheric attenuation/absorption associated with frequency operation beyond 30GHz, high gain antenna and/or antenna configuration arrays are an extensively used approach to compensate the path losses[2][5]. However, the use of a bulky dielectric lens placed on the top/bottom of the antennas is still required to improve the directivity[6]. As such a large geometry transceiver circuit will face integration difficulties into the mobile unit. Additional drawback also emerges from the very low mm-wave incident power at the receiver, necessitating that impedance matching between the integrated rectifier circuit and the antenna is of vital importance.

The work reported here concentrates on the design and theoretical analysis of a compact and relatively high gain folded antenna operating in the mm-wave regime. The attractive feature of the proposed folded antenna for high

frequency operation is laid out on the monolithically integration capability with rectifier circuits. This is primarily carried out without the need for matching circuits as the antenna geometry can be slightly modified to match the input impedance of the subsequent circuit. The antennas were simulated utilizing CST-Microwave Studio software by which low/high frequency antennas were built on 600 μ m thick semi-insulating GaAs substrate.

II. ANTENNA STRUCTURE AND EXPERIMENTAL RESULTS

The simulation was firstly performed at 7, 8 and 10GHz followed by fabrication using a conventional i-line photolithographic and wet etching process. Fig. 1 depicts the modeled and photomicrograph of a fabricated 8GHz antenna structure. The low frequency antenna designs were used to validate the simulation procedure followed here. The modeled and experimental return loss data show good agreement in terms of resonant frequency and >100MHz bandwidth as illustrated in Fig. 2. A similar finding has been also obtained for the 7, 9 and 10GHz antenna designs. As expected, the very small antenna's ultimate size of 1 \times 3mm² has come at the expense of a low gain of -14.6dB.

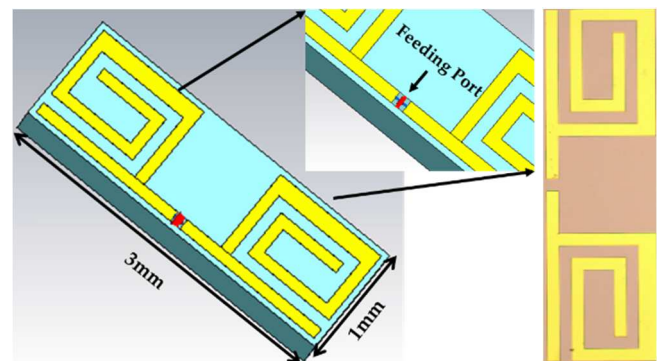


Fig. 1. Simulated (left-hand side) and fabricated (right-hand side) antenna structures designed to resonate at 8GHz.

An ASPAT (Asymmetric spacer layer tunnel diode) device sample XMBE#421 with a 10ML barrier thickness was to be integrated with the antenna. The equivalent circuit parameter extraction of the tunneling devices has been extensively investigated and reported previously[7][8]. The procedure carried out is based on the experimental S-parameter data obtained using a Vector Network Analyzer (VNA, Anritsu 37369A) up to 40GHz. A short-open-load-thru (SOLT) calibration method was used prior to on-wafer

probing technique to eliminate systematic errors for reliable and repeatable measurements.

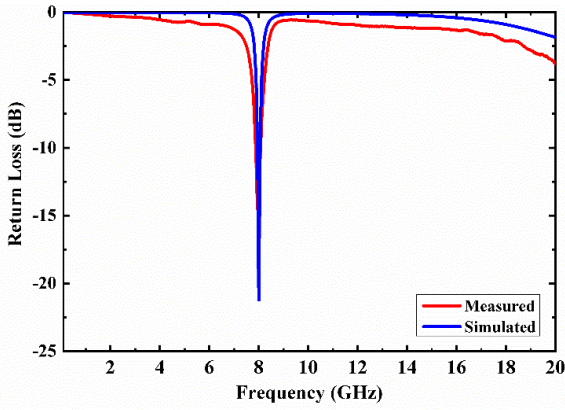


Fig. 2. Return loss response for the 8GHz folded antenna design.

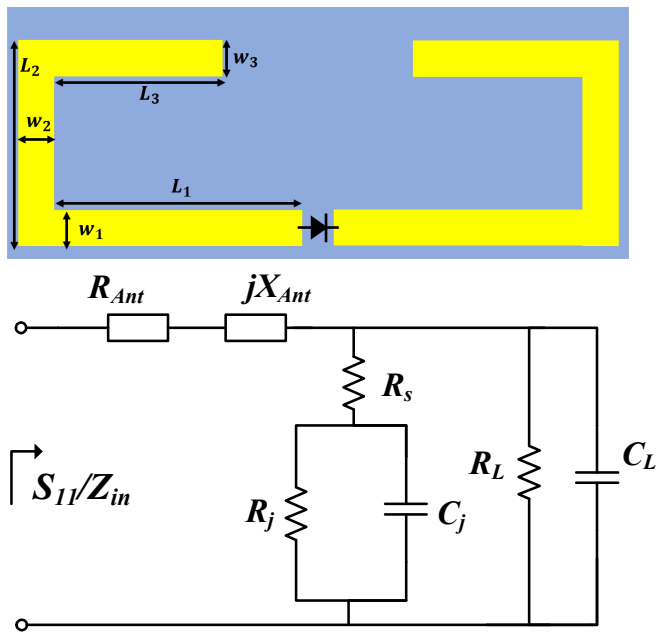


Fig. 3. Folded antenna structure along with integrated diode (top) and equivalent circuit model of the antenna and ASPAT diode and RC filter.

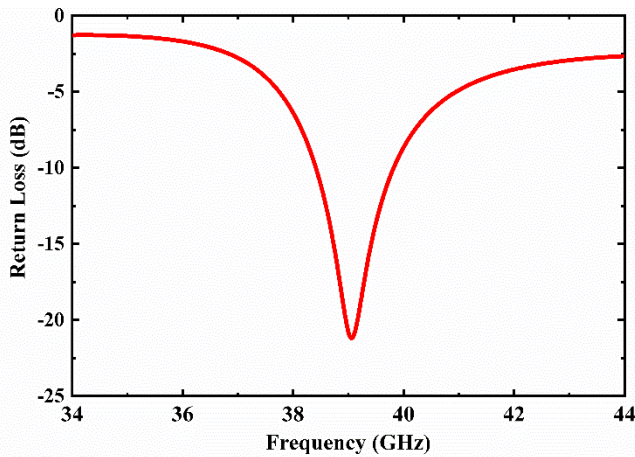


Fig. 4. Simulated return loss response for the folded antenna designed in this work.

The extracted junction resistance (R_j), junction capacitance (C_j) and series resistance (R_s) of a $6 \times 6 \mu\text{m}^2$

ASPAT device are $30\text{k}\Omega$, 91fF and 19Ω respectively. These provide a maximum operating frequency of 92GHz , which can be extended to higher frequencies by downscaling the device geometry. Fig. 3 shows the structure of the folded antenna including the length (L_1 , L_2 and L_3) and width (W_1 , W_2 and W_3) of the arms alongside the equivalent circuit model for the fully integrated rectenna circuit. The R_L and C_L are used to pick up the DC voltage component at the output termination. Of course, the higher R_L the higher output voltage is obtained. The validated results of the antenna structure were extended into frequencies beyond 30GHz with a resonant frequency of 39GHz as depicted in Fig. 4. The antenna has dimensions of $5 \times 10\text{mm}^2$ with a respective gain and directivity of 3.5dB and 4.6dBi with a frequency bandwidth of 780MHz . The mathematically expressed input impedance of the ASPAT diode is given by:

$$Z_{in(ASPAT)} = R_s + \frac{1}{1 + \omega^2 C_j^2 R_j^2} - j \frac{\omega C_j R_j}{1 + \omega^2 C_j^2 R_j^2} \quad (1)$$

Distinctly, the junction capacitance determines the reactance of the diode and series resistance is mostly affecting the real part of the device. From equation (1), the diode exhibits a capacitive behavior which varies with frequency as expected. The antenna input impedance (Z_{Ant}) can match the integrated diode at a certain frequency when the real part of both elements is comparable and the reactance condition is satisfied:

$$\left| jX_{Ant} - j \frac{\omega C_j R_j}{1 + \omega^2 C_j^2 R_j^2} \right| = 0 \quad (2)$$

The dependency of Z_{Ant} on the frequency provides a capacitive and inductive response at different frequencies. It is of vital importance to pointing out that C_j is dominated by the epi-layer structure and mesa size of the device. The simple approach is thus to optimize Z_{Ant} to get it matched with $Z_{in(ASPAT)}$ without the need for an associated matching network.

III. FURTHER OPTIMIZATION AND DISCUSSION

It is observed that the variation in the main antenna's arm width, W_1 has a significant impact on the real part while minimally affecting the imaginary part of the Z_{Ant} . In the same manner, the secondary arm width, W_3 plays a pivotal role in determining the reactive value of the Z_{Ant} , allowing to independently optimize R_{Ant} and jX_{Ant} of the folded antenna as shown in Fig. 5. The peak of R_{Ant} drops from nearly 600 to 200Ω at W_1 of 35 and $150\mu\text{m}$ respectively, attributed to the smaller resistance associated with wider antenna arms. This was carried out when the W_2 and W_3 were maintained at 40 and $500\mu\text{m}$ respectively, thus the impact of one parameter is investigated at a time. It is well-known that the lengths L_1 , L_2 and L_3 determine the resonant frequency of the antenna. The inductive behavior, jX_{Ant} of the antenna occurs at lower frequencies when the W_3 width increases as observed in Fig. 5. The $6 \times 6 \mu\text{m}^2$ ASPAT tunneling device has an input impedance, $Z_{in(ASPAT)}(\Omega) = 16 - j32$ at 39GHz . The optimized Z_{Ant} was found for W_1 and W_3 both equal to $20\mu\text{m}$ and the resonant frequency is shifted to 37.5GHz , which is still within the 5G mm-wave candidate frequency bands. Fig. 6. shows the simulated return loss result representing the matching response between the antenna and ASPAT diode. Despite of the fact that folded antennas have been previously demonstrated[9], this work covers the optimization procedure

with relevant analysis. The ability to miniaturize the ultimate size of the folded antenna through folding the arms accompanied by manipulating R_{Ant} and jX_{Ant} are invaluable features for mass produced, compact and cost effective rectenna integrated circuits.

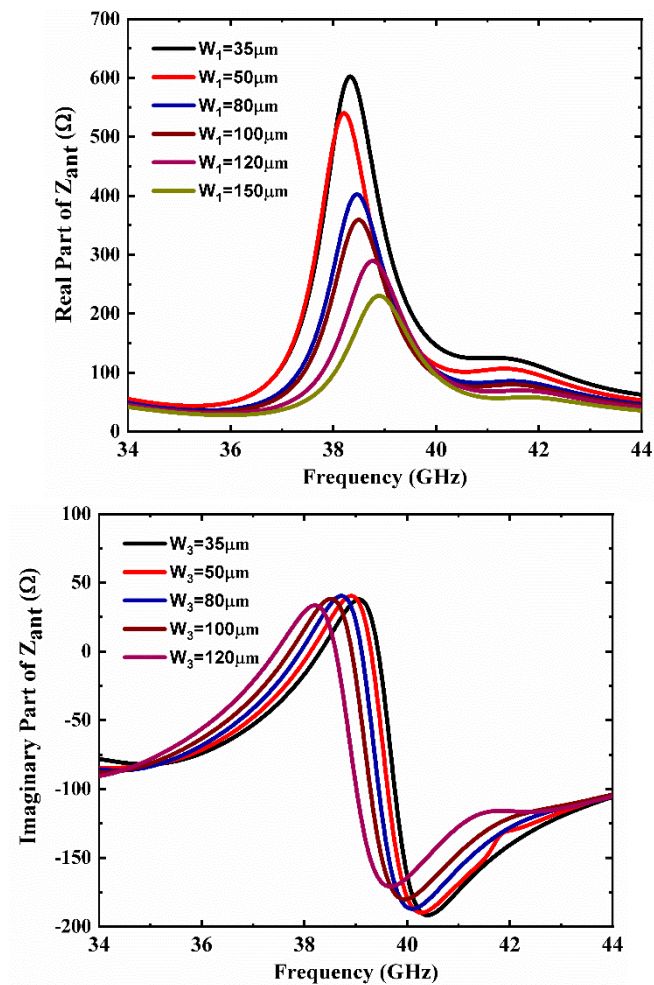


Fig. 5. Simulated real (top) and imaginary (bottom) parts of the Z_{Ant} with variation in W_1 and W_3 for the 39GHz folded antenna.

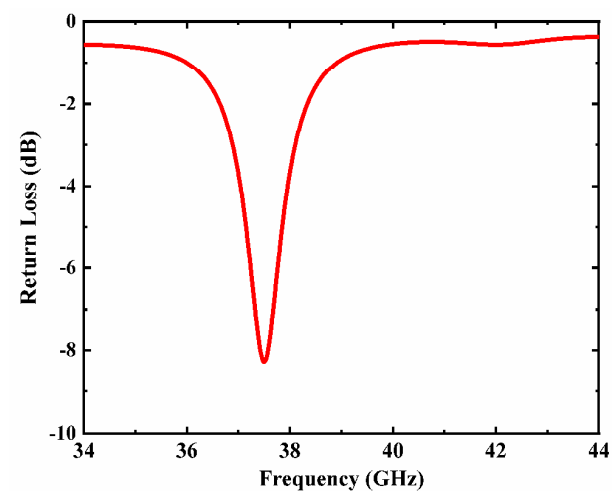


Fig. 6. Return loss matching response between $5 \times 10 \text{mm}^2$ folded antenna and $6 \times 6 \mu\text{m}^2$ ASPAT device sample X421.

IV. CONCLUSION

This paper presents a design and detailed optimization method for a folded antenna and zero bias ASPAT rectifier simulated using CST-Microwave Studio software. Low frequency operation antennas $\leq 10 \text{GHz}$ were utilized to validate the approach conducted here which exhibited excellent agreement with the experimental data. A mm-wave frequency of 39GHz folded antenna was built with a respective gain and directivity of 3.5dB and 4.6dBi aimed for 5G applications. It was found that the variation in W_1 and W_3 can contribute to optimize the input impedance of the antenna for matching to the ASPAT rectifier avoiding the need for a separate matching circuit and greatly simplifying the design of integrated rectenna circuits. This paves the way towards mass produced, efficient and cost effective rectenna circuits for mm-wave frequency applications

ACKNOWLEDGMENT

The authors thank Engineering and Physical Sciences Research Council (EPSRC) for supporting this work through EP/P006973/1 “Future Compound Semiconductor Manufacturing Hub”).

REFERENCES

- [1] N. Oshima, K. Hashimoto, S. Suzuki, and M. Asada, “Wireless data transmission of 34 Gbit/s at a 500-GHz range using resonant-tunnelling-diode terahertz oscillator,” *Electron. Lett.*, vol. 52, no. 22, pp. 1897–1898, 2016.
- [2] H.-C. Huang, “Overview of antenna designs and considerations in 5G cellular phones,” in *2018 International Workshop on Antenna Technology (iWAT)*, 2018, pp. 1–4.
- [3] H.-C. Huang, Y. Wang, and X. Jian, “Novel integrated design of dual-band dual-polarization mm-wave antennas in non-mm-wave antennas (AiA) for a 5G phone with a metal frame,” in *2019 International Workshop on Antenna Technology (iWAT)*, 2019, pp. 125–128.
- [4] T. S. Rappaport *et al.*, “Millimeter wave mobile communications for 5G cellular: It will work!,” *IEEE access*, vol. 1, pp. 335–349, 2013.
- [5] B. T. Malik, V. Doychinov, S. A. R. Zaidi, I. D. Robertson, and N. Somjit, “Antenna gain enhancement by using low-infill 3D-printed dielectric lens antennas,” *IEEE Access*, vol. 7, pp. 102467–102476, 2019.
- [6] T. Jäschke, B. Rohrdantz, H. K. Mitto, and A. F. Jacob, “Ultrawideband SIW-fed lens antenna,” *IEEE Antennas Wirel. Propag. Lett.*, vol. 16, pp. 2010–2013, 2017.
- [7] K. N. Z. Ariffin *et al.*, “Investigations of asymmetric spacer tunnel layer diodes for high-frequency applications,” *IEEE Trans. Electron Devices*, vol. 65, no. 1, pp. 64–71, 2017.
- [8] S. G. Muttalak, O. S. Abdulwahid, J. Sexton, M. J. Kelly, and M. Missous, “InGaAs/AIAs resonant tunneling diodes for THz applications: an experimental investigation,” *IEEE J. Electron Devices Soc.*, vol. 6, pp. 254–262, 2018.
- [9] Z. Wang, J. Wu, Y. Yin, and X. Liu, “A broadband dual-element folded dipole antenna with a reflector,” *IEEE Antennas Wirel. Propag. Lett.*, vol. 13, pp. 750–753, 2014.